

Supporting Information

The Dynamics of a Molecular Plug Docked onto a Solid-State Nanopore

Xin Shi¹, Qiao Li¹, Rui Gao¹, Wei Si^{2,3}, Shao-Chuang Liu¹, Aleksei Aksimentiev² and Yi-Tao Long^{*1}

1. Key Laboratory for Advanced Materials, School of Chemistry & Molecular Engineering, East China University of Science and Technology, Shanghai 200237 (P.R. China)

* E-mail: ytlong@ecust.edu.cn

2. Department of Physics, University of Illinois at Urbana–Champaign, 1110 W Green St, Urbana, IL 61801, USA

3. Jiangsu Key Laboratory for Design and Manufacture of Micro-Nano Biomedical Instruments and School of Mechanical Engineering, Southeast University, Nanjing 210096, P. R. China

Supplementary Method 1. Fabrication of sub-5nm by Controlled Dielectric Breakdown

The sub-5 nm solid-state nanopores were fabricated by controlled dielectric breakdown as demonstrated in the literature¹. Free-standing SiN film with thickness of 10 nm supported on a silicon frame (Norcada, Canada) was mounted in a liquid cell, separating two reservoirs with 1M KCl buffered to pH 8 with 10mM Tris-HCl and 1mM EDTA as electrolyte. The bias voltage across the membrane was applied via a pair of Ag/AgCl electrodes connected to a lab-made circuit, controlled by analogue data acquisition board (PCI-6251, National Instruments). The breakdown voltage was set constantly with a typical value as 7.5 V, which would be adjusted according the leakage current. The leakage current under 7.5 V with our experimental condition is typically 10-50 nA. A threshold of current was set according to the expected nanopore size, estimated by the pore conductance based on a cylindrical pore model, as Equation S1^{2,3}

$$G = \sigma \left[\frac{4l}{\pi d^2} + \frac{1}{d} \right]^{-1} \quad (\text{Equation S1})$$

Figure S1 shows typical current trace during the fabrication. A rapid current increase caused by the breakdown event could be observed, indicates the initial formation of the nanopore. After the breakdown, we hold the DC voltage which induce the continuously increasing of the ionic current, indicates the enlargement of the nanopore, until the current reach the set threshold. Once the nanopore with desired pore size is obtained, the lab-built circuit would be replaced by a commercial low-current amplifier (Axopatch 200B, Molecular Devices, US) then the open pore current under experimental bias voltages and the I-V curve could be measured. If the open pore current was stable under experimental potential and the I-V curve was linear, the nanopore could be used for the further experiments. Otherwise, following procedures would be applied to improve the nanopore condition: 1) replace the electrolyte into 4M LiCl and soak the whole device in the 1M LiCl solution overnight (>12 h) if the open pore current is not stable or the Root-Mean-Square (RMS) of open pore current is larger than tolerance (20 pA under 10 kHz bandwidth typically) or the I-V curve is asymmetry and linear; 2) apply a square wave voltage pulse to enlarge the nanopore till the expected nanopore size is reached. It should be noticed that in some cases, after the treatments mentioned above, the quality of certain nanopore devices might still cannot meet the requirement of the experiments. In this case, those nanopore chips will not be used for the further experiments. The final pore size would be estimated by the conductance measurement based on Equation ES1 or/and transmission electron microscopy (TEM). We also noticed that the fabrication time, noise level of nanopores, and success rate of controlled dielectric breakdown, under our

experimental condition highly affected by the quality of SiN membrane and a differences between batches is obviously existed.

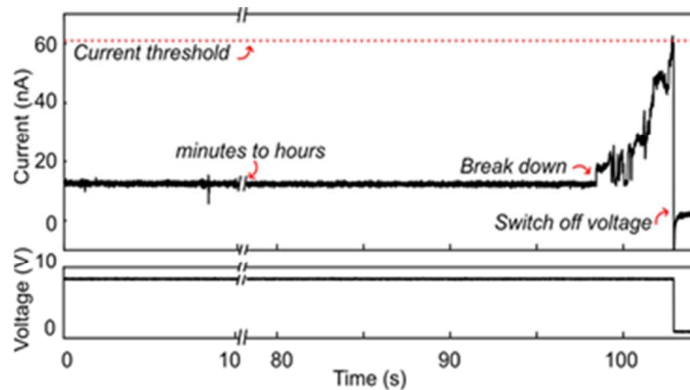


Figure S1. Typical current and voltage traces during the dielectric breakdown process, amplified with the lab-made current amplifier with 1 kHz bandwidth and digitized with a NI DAQ card. Real Time current recording and voltage control is executed with a LabVIEW program.

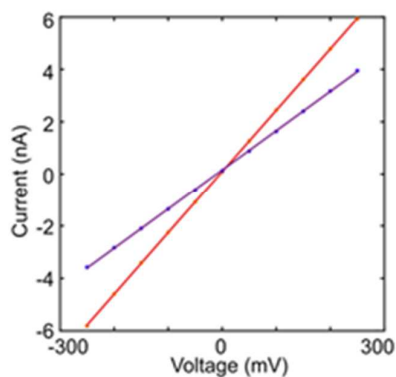


Figure S2. Typical IV curves of solid state nanopores fabricated by controlled dielectric breakdown.

Supplementary Method 2. Reversible trapping Monovalent streptavidin-tethered DNA:

The monovalent streptavidin and biotinylated DNA with a concentration of 200 nM are mixed in 1:1 ratio. Then incubate the mixture in room temperature for at least 5 min before adding into the grounded cis chamber of the nanopore flow cell. The volume of electrolyte in each chamber is $200\text{ }\mu\text{L}$ and the final concentration of the protein-DNA complex on the flow cell chamber is 5 nM . The applied bias voltage protocol is shown in Figure 1. It should be noticed that due to the slightly different capture rates caused by the nanopores' size, the final concentration of analyte would be adjusted by the addition of extra electrolyte or analyte, to maintain a high ratio of cycles with trapped molecules, and a clear segment of open-pore current before trapping to show the nanopore was cleared, as typical examples shown in Figure 1 in the main text. All the data in this work was processed and plotted with Matlab. All-points histograms of blockade current only include the current trace at last 2 sec before flipping voltage to avoid the artificial caused by the charging effect. All the histograms are normalized into probability (area=1).

ds-DNA: 3`-biotin-TEG - **TAC TTG ATC TGA ATA GGG ATT ACG AAA TGC ACA
ACA AGA GTT AGA GTG ATT TTG TCT TCC AAC TAT AAG CAA GTC CAG
TCA GTT GAG ACG**

and its complementary strand without the biotin tag.

22nt ss-DNA: 3`-biotin - TEG - **CCC TAA CCC TAA CCC TAA CCC T**

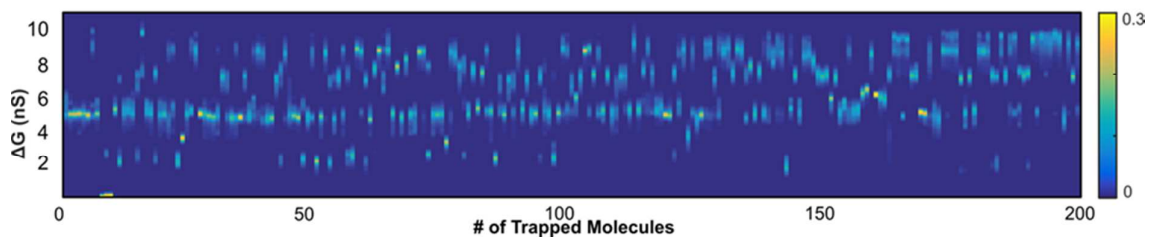


Figure S3. Additional examples of the ionic current fluctuation caused by docking dsDNA-streptavidin onto solid state nanopores. Same as Figure 2b, 200 all-points-histograms of dsDNA tethered streptavidin is plotted as heat map.

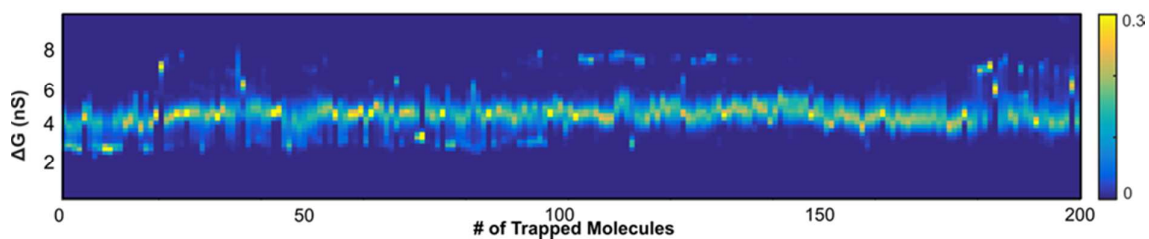


Figure S4. Additional examples of the ionic current fluctuation caused by docking ssDNA-streptavidin onto solid state nanopores. Same as Figure 2d, 200 all-points-histograms of ssDNA tethered streptavidin is plotted as heat map.

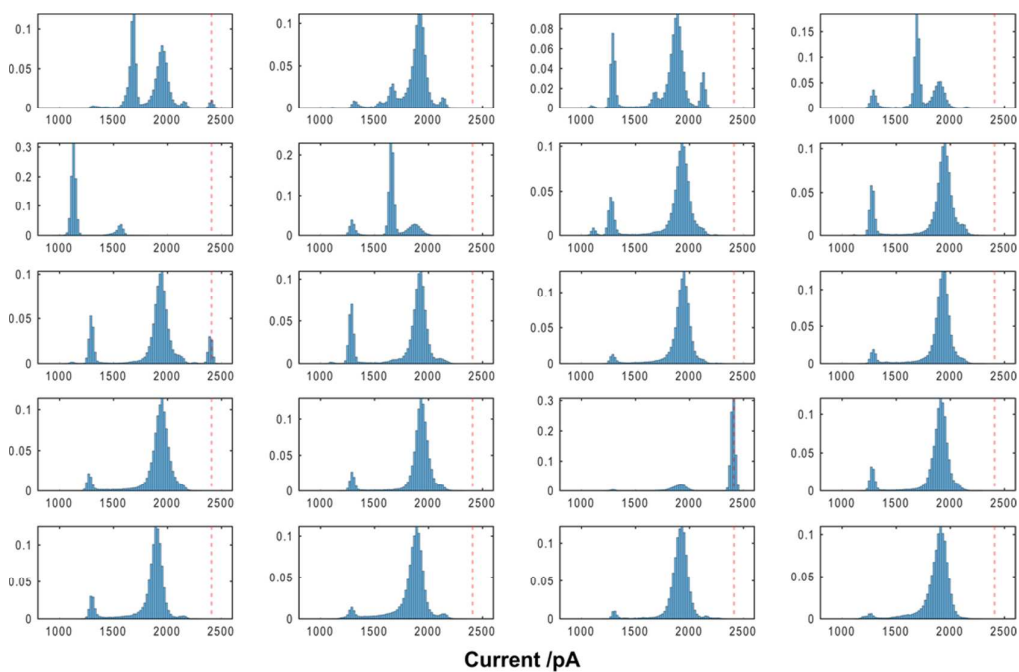


Figure S5. Additional all-points histogram of the ionic current fluctuation caused by docking ssDNA-streptavidin onto solid state nanopores. The red dash line indicates the open-pore current.

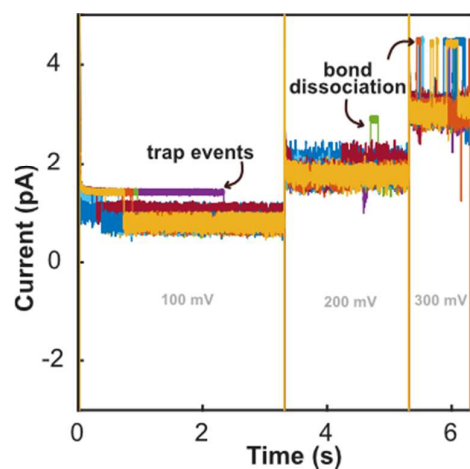


Figure S6 Rupture of a streptavidin-biotin bond as a function of voltage. The applied bias voltage is marked in the figure. Streptavidin-dsDNA complexes are captured and docked on the nanopore under 100 mV, producing distinguishable blockade current. Following that, the voltage is increased to 200 mV and 300 mV. Under 200 mV bias, a small number of streptavidin-biotin bond ruptures can already be observed. Under 300 mV, the ruptures are more frequent. The complexes are released by applying a -200-mV voltage.

Supplementary Method 3. Details of the blockade current calculation

Ionic current blockade produced by the presence of the streptavidin inside the nanopore was computed using a theoretical model described elsewhere⁴. The nanopore dimension as well its shape were adjusted to match the experimental open pore current within the experimental error. First, the streptavidin was placed above the nanopore and gradually moved toward the centre of the nanopore. The schematic illustration of the movement of the streptavidin and the respective current are shown in Figure S8. To avoid overlapping between the streptavidin and the nanopore wall, the streptavidin was finally placed 23 Å above the nanopore contraction and was randomly rotated while constraining its center of mass. For each orientation of the protein, we computed a 3D distance map at 1 Å resolution that specified the nearest distance to the protein or nanopore surface. The distance map was used to compute local ionic conductivity within pore; the pore's conductance was then determined by applying the Ohm law.

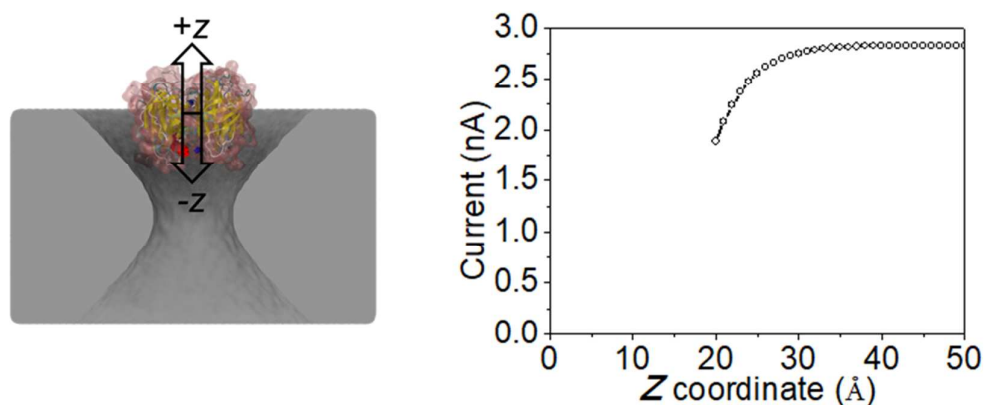


Figure S7. Calculated current modulation caused by moving the centre of mass of the streptavidin along the pore axis.

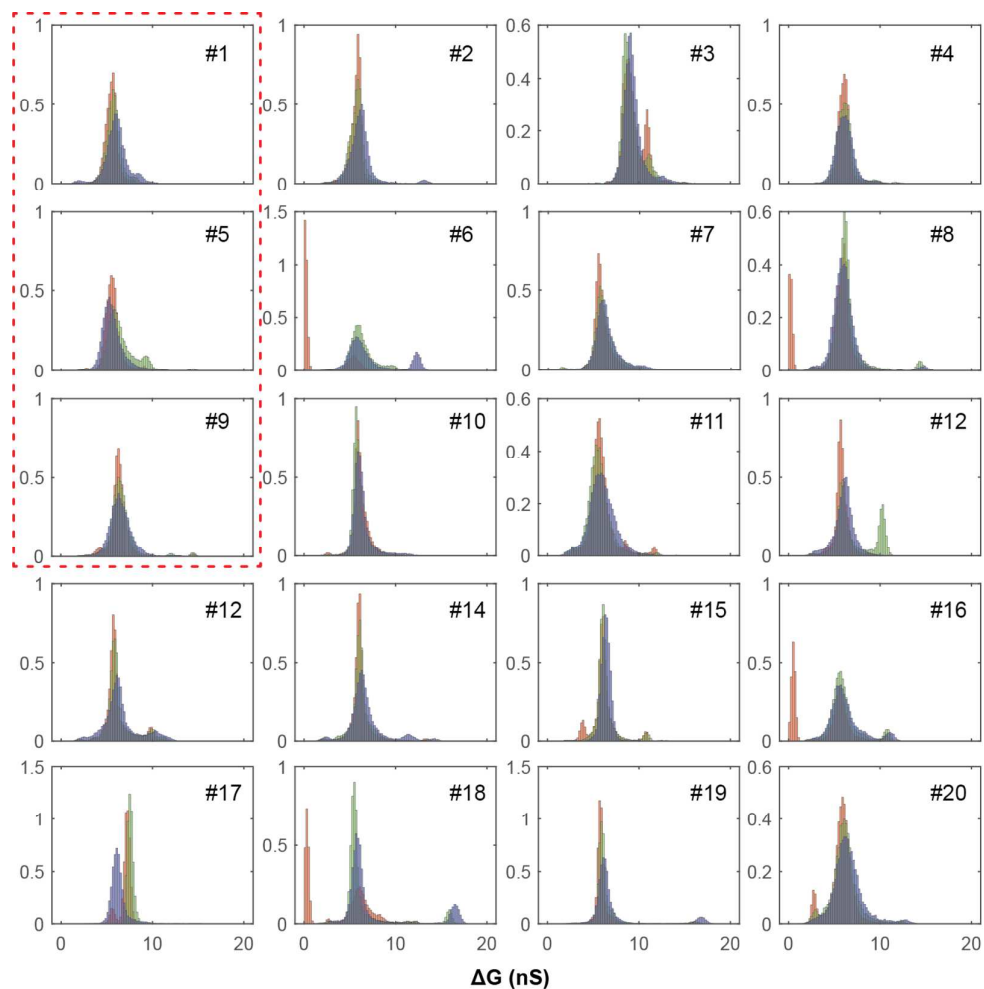


Figure S8. Additional all-points histogram of the ionic current blockades caused by same streptavidin-poly(dC)₉₀ complexes under different bias. Red: 100 mV, green: 75 mV, and blue: 50mV.

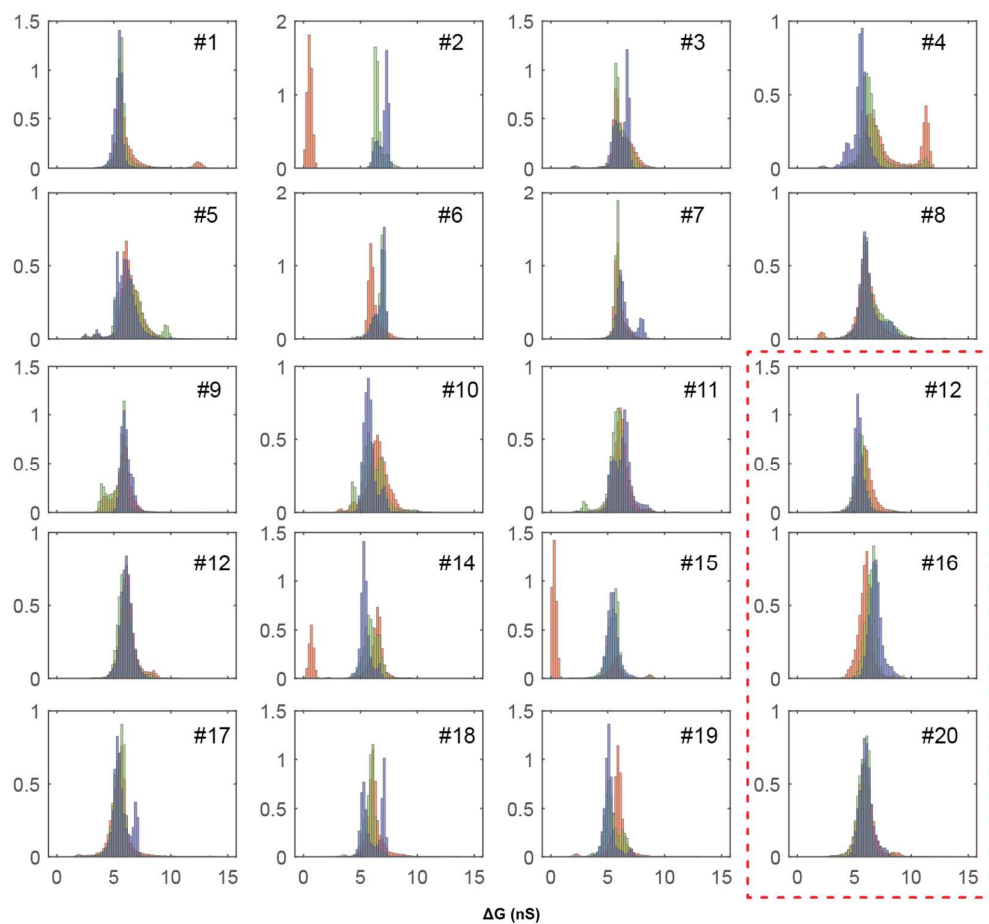


Figure S9. Additional all-points histogram of the ionic current blockades caused by same **streptavidin-poly(dC)₉₀** complexes under different bias. Red: 100 mV, green: 150 mV, and blue: 200mV.

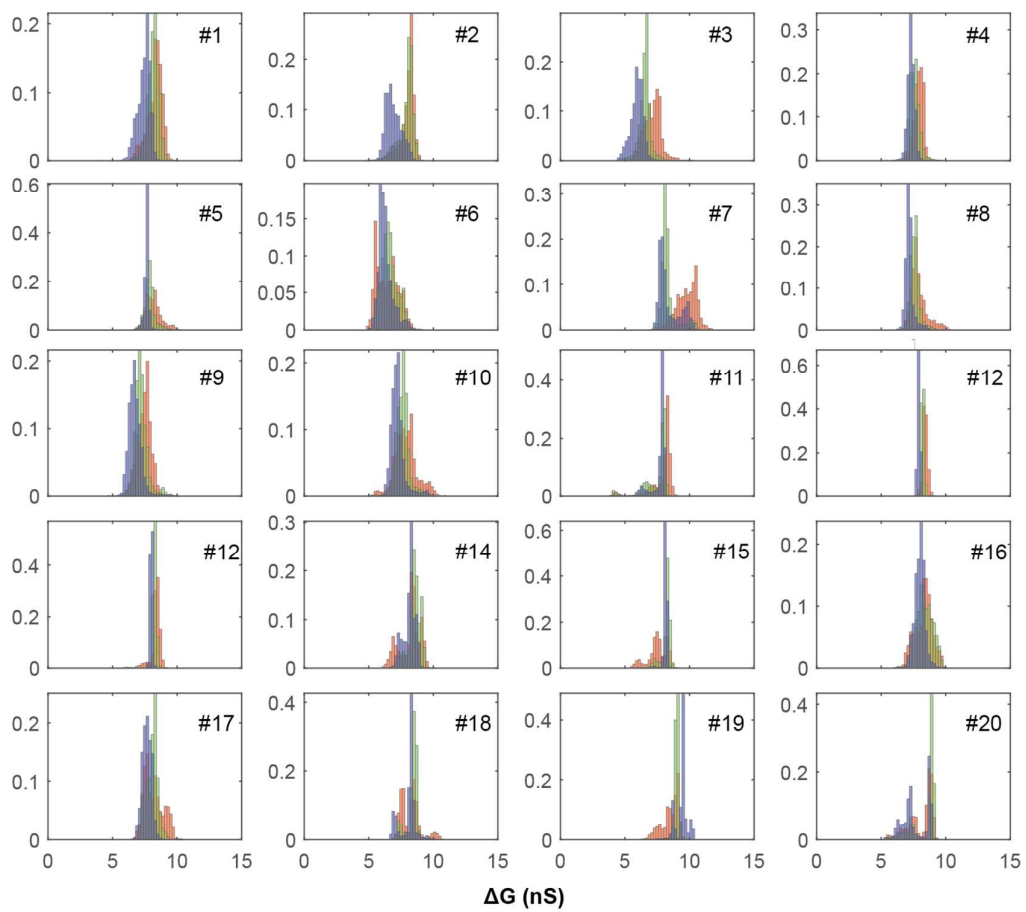


Figure S10. Additional all-points histogram of the ionic current blockades caused by same **streptavidin-dsDNA** complexes under different bias. Red: 100 mV, green: 150 mV, and blue: 200mV.

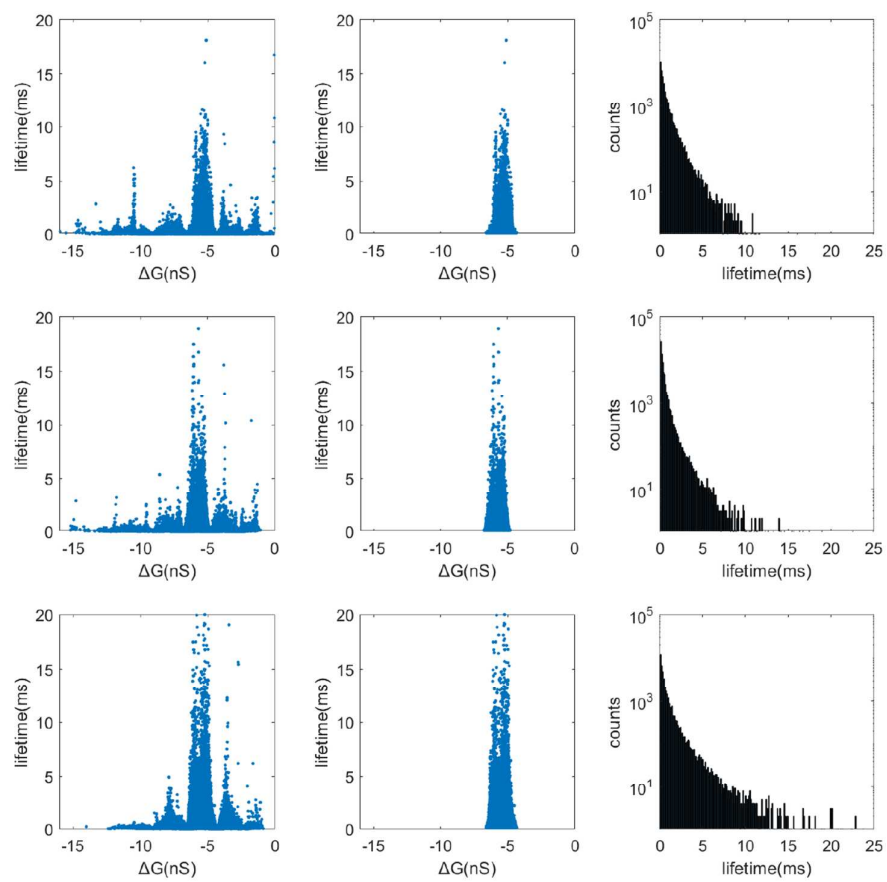


Figure S11. Lifetime analysis of current states produced by 100 streptavidin-poly(dC)₉₀ molecules under 100 mV, 150 mV, and 200 mV (from top panel to the bottom). Left column: scatter plots of lifetime of states vs ΔG analysed with Clampfit (Molecular Devices). Middle column: the most populated clusters in each case. Right column: histograms of the lifetime of the most populated level in each case.

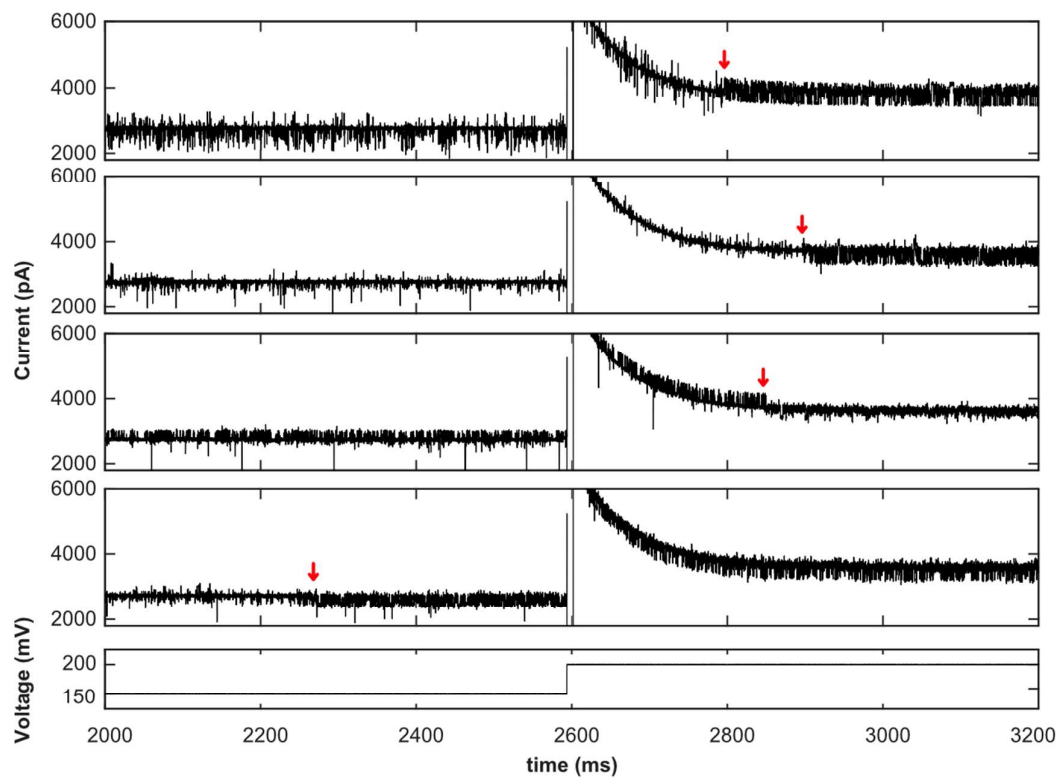


Figure S12. Examples of the changes of fluctuation pattern happen (red arrows) regardless the voltage changes.

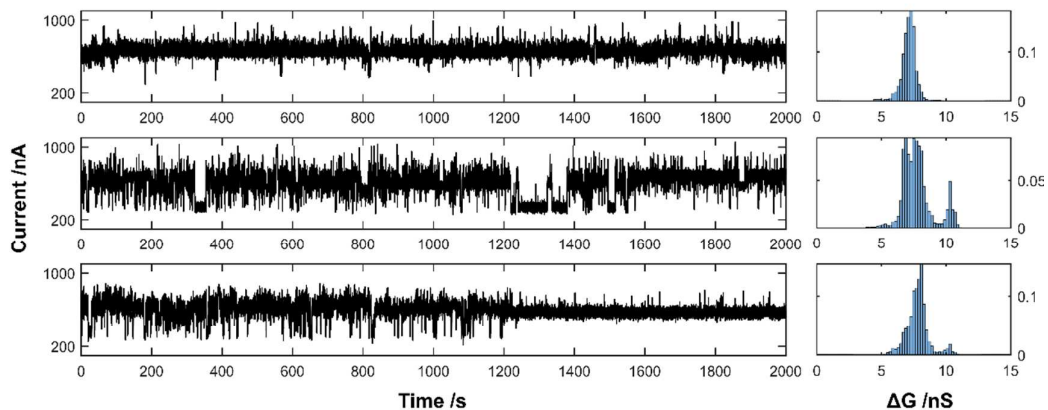


Figure S13. Typical current traces and corresponding all-points histograms of **streptavidin-dsDNA** docking events in pH 5 buffer.

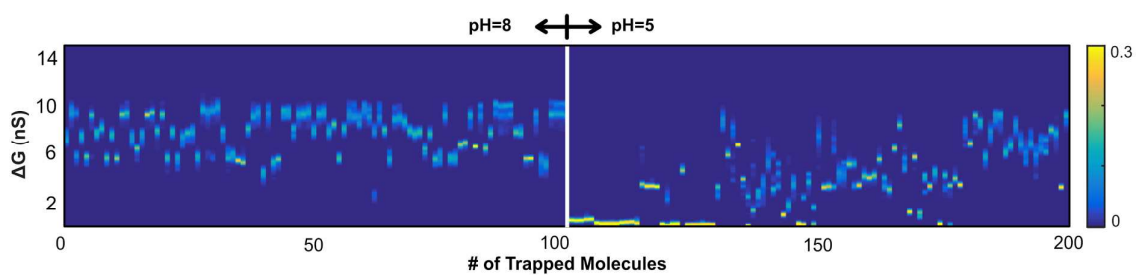


Figure S14. All-points histograms of current traces from **dsDNA-streptavidin** complexes docking in pH 8 and pH 5.

Supplementary Method 4. SS-DNA conformational changes by forming i-motif structures

Similar with the experiments of dsDNA and ssDNA above, the short c-rich ssDNA with biotin labels were attached to monovalent streptavidin by mixing them in 1:1 ration. The docking experiments are usually performed in the pH 8 buffer. The i-motif structures of ssDNA were formed by simply replace the electrolyte with 1 M KCl buffered to pH5 with acetate buffer. Then the same amount of protein-ssDNA complexes were added into the grounded chamber.

Reference

1. Kwok, H., Briggs, K. & Tabard-Cossa, V. Nanopore fabrication by controlled dielectric breakdown. *PLoS One* **9**, e92880 (2014).
2. Kowalczyk, S.W., Grosberg, A.Y., Rabin, Y. & Dekker, C. Modeling the conductance and DNA blockade of solid-state nanopores. *Nanotechnology* **22**, 315101 (2011).
3. Hyun, C., Rollings, R. & Li, J.L. Probing Access Resistance of Solid-State Nanopores with a Scanning-Probe Microscope Tip. *Small* **8**, 385-392 (2012).
4. Si, W. & Aksimentiev, A. Nanopore Sensing of Protein Folding. *ACS Nano* **11**, 7091-7100 (2017).